Microphysical Timescales in Clouds and their Application in Cloud-Resolving Modeling

Xiping Zeng

Goddard Earth Sciences and Technology Center, University of Maryland, Baltimore County, and Laboratory for Atmospheres, NASA Goddard Space Flight Center, Greenbelt, Maryland

Wei-Kuo Tao and **Joanne Simpson**

Laboratory for Atmospheres, NASA Goddard Space Flight Center, Greenbelt, Maryland

Submitted to *Journal of the Meteorological Society of Japan*

Popular Summary

With the continuous increase in computational power, cloud-resolving models will increase their domain size in the near future so that both clouds and large-scale circulations are simulated explicitly, addressing the role of clouds in weather and climate change. If a cloud model is coded in full modularization, scientists with various majors can develop or use the model for their research in parallel. Previous studies suggested that moist entropy be used as a prognostic variable for the separation (or modularization) of dynamics and thermodynamics. The present study shows how to tune prognostic variables for the separation (or modularization) of cloud microphysics and thermodynamics.

In this paper, microphysical timescales in clouds are surveyed in contrast to the time step for model integration, suggesting that moist entropy and total mixing ratio of airborne water without the contribution of precipitating particles be used as prognostic variables for the separation of cloud microphysics, thermodynamics and dynamics. Numerical simulations with these prognostic variables are compared with analytical solutions as well as simulations with conventional prognostic variables and shown to be efficient for modeling. The simulations also show that this method removes the prevalent computational phenomenon of spurious supersaturation and negative water in cloud-resolving modeling.

Microphysical Timescales in Clouds and their Application in Cloud-Resolving Modeling

Xiping Zeng*

Goddard Earth Sciences and Technology Center, University of Maryland, Baltimore County, and Laboratory for Atmospheres, NASA Goddard Space Flight Center, Greenbelt, Maryland

Wei-Kuo Tao and Joanne Simpson

Laboratory for Atmospheres, NASA Goddard Space Flight Center, Greenbelt, Maryland

Jan. 4, 2007

Submitted to *Journal of the Meteorological Society of Japan*

Corresponding author address: Dr. Xiping Zeng, Mail Code 613.1, NASA/Goddard Space Flight Center, Greenbelt, MD 20771. Email: zeng@agnes.gsfc.nasa.gov

Abstract

Independent prognostic variables in cloud-resolving modeling are chosen on the basis of the analysis of microphysical timescales in clouds versus a time step for numerical integration. Two of them are the moist entropy and the total mixing ratio of airborne water with no contributions from precipitating particles. As a result, temperature can be diagnosed easily from those prognostic variables, and cloud microphysics be separated (or modularized) from moist thermodynamics. Numerical comparison experiments show that those prognostic variables can work well while a large time step (e.g., 10 s) is used for numerical integration.

1. Introduction

With the continuous increase in computational power, cloud-resolving models will be extended to explicitly simulate clouds and synoptic large-scale circulations for their interaction in the near future. Since cloud microphysics is highly coupled with other processes, it is better for the models to represent properly not only individual clouds systems and large-scale circulations, but also cloud microphysics. Deep cumulus clouds in the Tropics act as an engine for the atmosphere, driving large-scale vertical circulations through convective heating (Riehl and Malkus 1958). Since the convective heating originates in the change of water phases on micro-scales, the "efficiency" of the engine is related to cloud microphysics (e.g., Simpson *et al.* 1988; Tao and Adler 2003a). On the other hand, small particles in clouds absorb and emit radiation that changes the atmospheric energy budget and in turn large-scale circulations (e.g., Albrecht and Cox 1975; Baker 1997). As a result, they are coupled with large-scale circulations (e.g., Raymond 2000; Raymond and Zeng 2000). Hence, it is interesting to represent cloud microphysics properly in long-term cloud-resolving modeling.

Cloud-resolving models consist of many parts: dynamics, moist thermodynamics, cloud microphysics, atmospheric radiation and the energy exchange between air and its underlying surface (e.g., Klemp and Wilhelmson 1978; Grabowski 1989; Tao and Simpson 1993; Tompkins and Craig 1998; Cotton *et al.* 2003; Tao *et al.* 2003b). They are becoming more and more complicated for various applications. Code modularization provides a suitable framework for a model to accommodate many parts so that different scientists can test or develop a part (e.g., cloud microphysics) on parallel. Ooyama (1990,

2001) first proposed the separation (or modularization) of dynamics and moist thermodynamics by choosing suitable prognostic variables. He suggested moist entropy and the mixing ratio of water substance be used as prognostic variables and temperature be diagnosed from those and other prognostic variables. He constructed a two-dimensional model for warm clouds to show the possibility of his proposal (Ooyama 2001). Moving in the same direction, the present paper proposes the separation (or modularization) of cloud microphysics and moist thermodynamics by tuning prognostic variables, especially for the modeling of cold clouds.

Moist entropy (or entropy-like variables), as other threads, was used as a prognostic variable in cloud modeling for other purposes. Tripoli and Cotton (1981, 1982) first used an entropy-like variable (or ice-liquid water potential temperature) as a prognostic variable in modeling to avoid a computational phenomenon or the negative mixing ratio of cloud water. Raymond and Blyth (1986) used moist entropy and the mixing ratio of airborne water (water vapor and cloud water) as prognostic variables in a parcel model to study cloud mixing. Zeng (2001) used moist entropy as a prognostic variable in a three-dimensional model for the ensemble simulation of warm clouds. Zeng *et al.* (2005) derived a precise equation for moist entropy so that moist entropy can work as a prognostic variable in cold-cloud modeling. The present paper, on the basis of the analysis of microphysical timescales in clouds, tunes prognostic variables for the separation of cloud microphysics and moist thermodynamics as follows: the contributor to moist entropy is changed from water substance (Tripoli and Cotton 1982; Ooyama 1990, 2001) to airborne water (or water substance except for precipitating water) and the use of moist entropy as a prognostic variable is extended from the simulation of warm

clouds (Raymond and Blyth 1986; Ooyama 1990, 2001; Zeng 2001) to the simulation of cold clouds.

Two issues need to be cleaned before moist entropy is used as a prognostic variable to simulate *cold* clouds. One issue is on the entropy budget equation (Tripoli and Cotton 1981; Ooyama 1990) that involves the irreversible generation of moist entropy. Zeng *et al.* (2005) derived an accurate entropy equation from the energy equation, expressing explicitly the irreversible generation of moist entropy due to cloud microphysics.

The other issue is on the benefit for the use of moist entropy as a prognostic variable. Ooyama (1990, 2001) chose moist entropy as a prognostic variable for the simulation of warm clouds since it is conservative. However, moist entropy is not conservative in cold clouds because ice usually brings about the irreversible generation of moist entropy (e.g., Zeng *et al.*, 2005). Thus, the benefit should be specifically explored before moist entropy is used as a prognostic variable in the simulation of cold clouds.

The present paper addresses the latter issue as follows. Section 2, with the aid of a simple example, illustrates a computational phenomenon of cloud microphysics in cloud-resolving modeling, proposing a strategy for code modularization of cloud microphysics. Section 3 compares the timescale for water vapor condensation with a time step in a non-precipitating parcel model for warm clouds, showing how the use of moist entropy as a prognostic variable benefits the separation (or modularization) of cloud microphysics and moist thermodynamics. Section 4 introduces a parcel model for cold clouds in terms of microphysical timescales and analyzes numerical results from the model, showing that moist entropy can work well as a prognostic variable in cold-cloud modeling. Section 5

gives a summary. Except for special illustrations, the paper follows the symbol definitions in Appendix A.

2. Code modularization of cloud microphysics

If all prognostic variables in a model are independent and they are integrated explicitly, code can be modularized fully. Using a simple example, this section illustrates a strategy for the modularization of cloud microphysics in cloud-resolving modeling.

Many cloud microphysical processes can be described with a simple equation that looks like (see sections 3 and 4 for details)

$$d\phi/dt = -\phi/\tau, \tag{2.1}$$

where the variable ϕ is a function of time t and the characteristic timescale τ is constant. Suppose that ϕ=1 at t=0. Thus, Equation (2.1) is solved analytically with $\phi = \exp(-t/\tau)$.

Although the preceding equation is very simple and its numerical schemes have been discussed in some textbooks, a brief survey is given here on its numerical schemes for a quick reference. Suppose that Equation (2.1) is discretized as

$$\phi^{n+1} = \phi^n - \phi^n \Delta t/\tau \tag{2.2}$$

for explicit integration, where superscripts indicate time level and Δt is the time step for integration. Equation (2.2) is solved with $\phi^n = (1-\Delta t/\tau)^n$. Obviously, the numerical solution of (2.2) is close to the analytical solution of (2.1) when

$$\Delta t < \tau. \tag{2.3}$$

Otherwise, the value of ϕ^n blows up or oscillates spuriously around zero. The preceding stability criterion can be applied to the modeling of cloud microphysics (Khvorostyanov and Sassen 1998).

Alternatively, Equation (2.1) can be discretized as

$$\phi^{n+1} = \phi^n - \phi^{n+1}\Delta t/\tau, \tag{2.4}$$

for implicit integration, which is solved with $\phi^n = (1+\Delta t/\tau)^{-n}$. Obviously, the numerical scheme in (2.4) is always stable, even when the time step is larger than the characteristic timescale.

Different from the preceding explicit and implicit schemes, the analytical solution of (2.1) can be approximated with

$$\phi^{n+1} = 0 \tag{2.5}$$

when the time step is larger than the characteristic timescale. In other words, Equation (2.1) degenerates from a prognostic equation into a diagnostic one.

In view of the numerical schemes in (2.2), (2.4) and (2.5) for the equation (2.1), it is reasonably inferred that cloud microphysics can be modularized fully when all independent prognostic equations for cloud microphysics take the similar numerical schemes as those in (2.2) or (2.5). That is, the explicit scheme in (2.2) or the approximation in (2.5) is used when the timescale of a process is larger or smaller than a given time step, respectively. Such strategy is taken in the following two sections for the modularization of cloud microphysics.

3. Choice of prognostic variables for warm-cloud modeling

This section compares two sets of prognostic variables for the modeling of non-precipitating warm clouds, showing the benefit for the use of moist entropy as a prognostic variable. To distinguish the two sets of prognostic variables clearly, it starts at the introduction of zero supersaturation approximation.

a. Two sets of prognostic variables

Consider an air parcel with monodisperse cloud droplets, as an example, where only cloud droplets evaporate or water vapor condenses on them. The concentration and the radius of droplets in the parcel are denoted with N_c and r_c, respectively. Thus, the mixing ratio of cloud water

$$q_c = \frac{4}{3}\pi\rho_w \frac{N_c}{\rho} r_c^3 . \tag{3.1}$$

The growth rate of a droplet due to water vapor condensation is expressed as (e.g., Pruppacher and Klett 1997)

$$\frac{dr_c}{dt} = \frac{A_w(q_v/q_{vsw} - 1)}{r_c}, \tag{3.2}$$

where q_v is the mixing ratio of water vapor, q_{vsw} the saturation mixing ratio of water vapor over water and

$$A_w = (\rho_w L_v^2 / K_a R_v T^2 + \rho_w R_v T / E_{sw} D_v)^{-1} . \tag{3.3}$$

Differentiating (3.1) with respect to time, and then substituting (3.2) into the resulting equation yields

$$\frac{dq_v}{dt} = -\frac{dq_c}{dt} = -4\pi\rho_w A_w r_c \frac{N_c}{\rho}\left(\frac{q_v}{q_{vsw}} - 1\right) . \tag{3.4}$$

Assume that the parcel is adiabatic and stationary (or zero vertical velocity). Thus, the energy equation is written approximately as

$$C_p \frac{dT}{dt} = -L_v \frac{dq_v}{dt} . \tag{3.5}$$

Substituting (3.4) into (3.5) yields

$$\frac{d(q_v - q_{vsw})}{dt} = -4\pi\rho_w A_w r_c \frac{N_c}{\rho}(1 + \frac{q_{vs}L_v^2}{R_v C_p T^2})\frac{q_v - q_{vsw}}{q_{vsw}} \tag{3.6}$$

with the aid of the Clausius-Clapeyron equation

$$\frac{d\ln E_{sw}}{dT} = \frac{L_v}{R_v T^2}. \tag{3.7}$$

The analogy between Equations (3.6) and (2.1) shows the timescale for water vapor condensation (or cloud water evaporation)

$$\tau = (1 + \frac{q_{vsw}L_v^2}{R_v C_p T^2})^{-1} \frac{\rho q_{vsw}}{4\pi\rho_w A_w N_c r_c} \tag{3.8}$$

which is consistent with that of Squires (1952), Politovich and Cooper (1988) and Korolev and Mazin (2003).

Figure 1 exhibits the timescale versus height, where the air density is approximated with that of a static atmosphere whose surface pressure is 1013.25 hpa and temperature decreases linearly with height from 288 at z=0 to 216.5 K at z=11 km. The thin and thick lines in the figure display the timescale against height when $N_c r_c$=500 and 3000 $\mu m \cdot cm^{-3}$, respectively. As noticed in the figure, the timescale for continental air is around 1 second and that for marine air is around 5 seconds.

If T, q_v and q_c are used as prognostic variables to integrate Equations (3.4), (3.5) and (3.6), the time step for explicit integration must be smaller than the timescale τ, just as shown in section 2. Thus, the time step is very small since the timescale may be 1 second or less.

Alternatively, if moist entropy and the mixing ratio of airborne water are used as prognostic variables, the time step is not limited by the timescale, which is discussed next. The moist entropy per unit mass of dry air is defined as the sum of entropies for

such constituents as dry air, water vapor, cloud water and ice. It is equivalently expressed as (Zeng *et al.* 2005)

$$s = (C_p + c_l q_t)\ln\frac{T}{T_{ref}} - R_d \ln\frac{p-e}{p_{ref}} + (\frac{L_v}{T} - R_v \ln f)q_v - (\frac{L_f}{T} - R_v \ln\frac{E_{sw}}{E_{si}})q_i, \quad (3.9)$$

where relative humidity $f=e/E_{sw}$; T_{ref} = 273.15 K and p_{ref} = 10^5 pa are the reference temperature and pressure, respectively; the total mixing ratio of airborne water (water vapor, cloud water and ice) is

$$q_t = q_v + q_c + q_i; \quad (3.10)$$

and the supersaturation of water vapor s_w is

$$s_w = (q_v - q_{vsw})/q_{vsw}. \quad (3.11)$$

When s, q_t and s_w are used as prognostic variables, their governing equations are

$$\frac{ds}{dt} = \frac{dq_t}{dt} = 0 \quad (3.12)$$

$$\frac{d(s_w q_{vsw})}{dt} = -\frac{(s_w q_{vsw})}{\tau}. \quad (3.13)$$

Since the timescale τ measures the adjustment of s_w to zero and its value is small, the approximation of zero supersaturation s_w=0, just like Equation (2.5), is introduced while water changes phase. As a result, three prognostic variables s, q_t and s_w are decreased to *two* prognostic ones (i.e., s and q_t), and the time step for explicit integration[1] is not limited by the small timescale τ.

[1] If the evolution of real supersaturation is interested (e.g., Khvorostyanov and Sassen 1998), s_w=0 can't be introduced. Thus, all of s, q_t and s_w are used as prognostic variables. As a result, the time step for explicit integration is limited by τ. However, this topic is beyond the present paper.

Summarily, when (T, q_v, q_c) are used as *independent* prognostic variables, real supersaturation is explicitly simulated and the time step for explicit integration is limited by the small timescale[2]. When (s, q_t) are used as independent prognostic variables and the approximation of zero supersaturation is introduced, the time step is not limited by the small timescale. Meanwhile, no real supersaturation is simulated well.

The approximation of zero supersaturation is supported by observations. Real supersaturation in clouds is usually calculated with observational data of temperature, vertical velocity and cloud droplets, since it can not be measured directly. It is found that real supersaturation in cumulus clouds is in the range from –0.5 to 0.5% and rarely exceeds 1% (Politovich and Cooper 1988).

b. Diagnosing temperature from moist entropy

When s and q_t are used as prognostic variables, temperature is diagnosed from them. The diagnosis procedure is summarized in the flow chart in Figure 2. For the sake of completeness, the diagnosis part for cold clouds is also presented in the figure for the further discussion in section 4.

---

[2] If (T, q_v, q_c) are used as prognostic variables to simulate a system with a constraint (or zero supersaturation), the timescale of cloud water evaporation does not limit the time step for explicit integration, since it does not exist in the system. However, *the three prognostic variables are not independent*. They are one more than necessary. As a result, numerical integration may violate the constraint, bringing about computational phenomena. Thus, special technologies (e.g., Grabowski and Smolarkiewicz 1990; Margolin *et al.* 1997) are needed to remove the computational phenomena.

Consider a hypothetical parcel with s the moist entropy, p the pressure and q_i the mixing ratio of cloud ice. The parcel stays right at water-saturation and contains no cloud water. Its temperature is denoted as T_w^* and its saturation mixing ratio of water vapor as

$$q_{vsw}^* = 0.622 \frac{E_{sw}(T_w^*)}{p - E_{sw}(T_w^*)}. \tag{3.14}$$

Using the preceding equation, Equation (3.9) is solved for T_w^* with the Newton iterative method first. Then, q_{vsw}^* is determined by (3.14).

Since the moist entropy and the mixing ratio of airborne water are conserved when water vapor condensates or cloud drops evaporate, q_{vsw}^* for the hypothetical parcel is compared with q_t-q_i for the original parcel, judging whether the original parcel is saturated with respect to water or not. If q_t-q_i<q_{vsw}^*, the air is unsaturated with respect to water. Thus q_c=0, q_v=q_t-q_i, and Equation (3.9) is solved for the air temperature T with the Newton iterative method. If q_t-q_i≥q_{vsw}^*, the air is saturated with respect to water. Thus q_v=q_{vsw}^*, T=T_w^* and q_c=q_t-q_v-q_i. Once ice is involved, next is to judge whether cloud water freezes due to homogeneous ice nucleation (see section 4.a for more discussion).

c. Result comparison in a parcel model

This subsection analyzes numerical results from a parcel model with two sets of prognostic variables. Consider an air parcel in adiabatic upward motion. Its governing equations are written as follows with one set of prognostic variables (T, q_v, q_c)

$$\frac{dq_c}{dt} = -\frac{dq_v}{dt} \tag{3.15}$$

$$(C_p + C_{pv}q_v + c_l q_c)\frac{dT}{dt} - R_d T \frac{d\ln(p-e)}{dt} - q_v R_v T \frac{d\ln e}{dt} = -L_v \frac{dq_v}{dt} \tag{3.16}$$

$$\frac{dp}{dt} = -\rho g w \tag{3.17}$$

and

$$\frac{dq_v}{dt} = -(1 + \frac{q_{vsw} L_v^2}{R_v C_p T^2})^{-1} \frac{q_v - q_{vsw}}{\tau} \tag{3.18}$$

when $q_v > q_{vsw}$ or $q_c > 0$. Otherwise, $dq_v/dt = 0$.

Of the preceding equations, Equation (3.17) is obtained from the hydrostatic equation, and (3.18) is obtained from (3.4) and (3.8). As shown in (3.8), the timescale τ changes with time. Its variation can be represented in spectral-bin models that explicitly simulate the spectrum of cloud drops (e.g., Khvorostyanov and Sassen 1998; Tao *et al.* 2003b). For simplicity, a constant timescale $\tau = 1$ s is used in (3.18) so as to bring computational phenomena into focus.

The governing equations for the parcel can be expressed with the other set of prognostic variables (s, q_t). They are (3.12) and (3.17), corresponding to those with the first set of variables. The parcel model takes the same numerical schemes as that in Equation (2.2).

Suppose that the air parcel moves upward with a vertical velocity of $w = 4$ m/s as well as an initial pressure 1000 hpa, relative humidity of 85% and temperature of 300 K. Numerical results from the model are displayed in Figure 3. The results from the model with $\Delta t = 0.1$ s and the first set of prognostic variables are displayed with thin solid lines. These results can be regarded as a benchmark to check the results in other experiments.

The results from the model with $\Delta t = 3$ s and the first set of prognostic variables are displayed with thin dashed lines in Figure 3. As shown in the figure, the results are bad compared to those with $\Delta t = 0.1$ s. Both spurious supersaturation and negative mixing ratio

of cloud water are present. When Δt=10 s is used, the model blows up due to computational instability. The results from the model with Δt=10 s and the second set of prognostic variables are displayed with thick dashed lines in Figure 3. As shown in the figure, the results agree well with those of the model with Δt=0.1 s and the first set of prognostic variables, and neither spurious supersaturation nor negative mixing ratio of cloud water is present. These numerical experiments clearly show that, if all prognostic variables are independent, moist entropy and the total mixing ratio of airborne water work more efficiently than temperature and the mixing ratios of water vapor and cloud water as prognostic variables in cloud-resolving modeling.

d. Result comparison in a one-dimensional model

This subsection analyzes numerical results from a one-dimensional model with two sets of prognostic variables, showing computational phenomena of a short timescale in a spatial model. Consider an idealized case in a one-dimensional space (Grabowski and Smolarkiewicz 1990). Air moves upward at a constant vertical velocity of 4 m/s. At the surface z=0, p=1013.25 hpa, T=288 K, f=30% and q_c=0. Initially, relative humidity is 30% except for 100% between z=1 and 2 km; temperature decreases linearly with height from 288 at z=0 to 216.5 K at z=11 km; and no liquid water exists.

When one set of prognostic variables (T, q_v, q_c) is used, the governing equations corresponding to (3.15), (3.16) and (3.18) are

$$\frac{\partial q_v}{\partial t} + w\frac{\partial q_v}{\partial z} = -(1+\frac{q_{vsw}L_v^2}{R_v C_p T^2})^{-1}\frac{q_v - q_{vsw}}{\tau} \tag{3.19}$$

$$\frac{\partial q_c}{\partial t} + w\frac{\partial q_c}{\partial z} = (1+\frac{q_{vsw}L_v^2}{R_v C_p T^2})^{-1}\frac{q_v - q_{vsw}}{\tau} \tag{3.20}$$

$$(C_p + C_{pv}q_v + c_l q_c)(\frac{\partial T}{\partial t} + w\frac{\partial T}{\partial z}) + \frac{\rho g R_d w T}{p - e} = L_v(1 + \frac{q_{vsw}L_v^2}{R_v C_p T^2})^{-1}\frac{q_v - q_{vsw}}{\tau} \qquad (3.21)$$

where the terms on the right hand side equal zeros while $q_v \le q_{vsw}$ and $q_c < 0$. The timescale τ=1 s is set for simplicity.

When the other set of prognostic variables (s, q_t) is used, the governing equations are obtained from (3.12), or

$$\frac{\partial s}{\partial t} + w\frac{\partial s}{\partial z} = 0 \qquad (3.22)$$

$$\frac{\partial q_t}{\partial t} + w\frac{\partial q_t}{\partial z} = 0 \qquad (3.23)$$

In all numerical experiments in this subsection, the uniform vertical grid size Δz=200 m is used. A traditional upstream scheme (e.g., Smolarkiewicz 1983) is applied to Equations (3.19)-(3.21). Following an air parcel in the model, it is easy to notice such computational phenomena as spurious supersaturation and negative mixing ratio of cloud water, just as shown in Figure 3, when a large time step (e.g., 3 seconds) is used (figure omitted). The spatial distribution of variables at t=10 minutes from the model is displayed in Figure 4, where solid and dashed thin lines show numerical results versus height when the time step Δt=0.1 and 3 s, respectively. Thick dashed lines show the corresponding analytical solution from (3.22) and (3.23) for comparison. As shown in the figure, the results with a small time step are close to the analytical ones, and the results with a large time step are bad.

The same traditional upstream scheme is applied to (3.22) and (3.23), and the numerical results at t=10 minutes from the model are shown in Figure 5, where thin solid lines show variables versus height when the time step Δt=10 s. As shown in the figure,

neither negative mixing ratio of cloud water nor spurious supersaturation is present, and the results are very close to those with Δt=0.1 s and the first set of prognostic variables in Figure 4. The difference between the numerical and the analytical results comes mainly from computational diffusion of the traditional upstream scheme, which is supported by the next experiment. The positive definite scheme of Smolarkiewicz (1983) has little computational diffusion in contrast to the traditional upstream scheme. It is applied to (3.22) and (3.23) with Δt=10 s. Its results are shown with thin dashed lines in the figure, showing that the numerical results are improved obviously. In brief, the numerical results in Figures 4 and 5 indicate that moist entropy can work well as a prognostic variable in a spatial model.

4. Microphysical timescales in cold-cloud modeling

This section addresses the modeling of cold clouds with moist entropy as a prognostic variable, and proposes introducing microphysical timescales as intermediate variables for the separation (or modularization) of cloud microphysics and moist thermodynamics. The section first compares the magnitudes of microphysical timescales with a time step (e.g., 10 s) for the choice of prognostic variables. Then, it introduces a parcel model for cold clouds expressed in terms of microphysical timescales. Finally, it analyzes numerical results from the model with two sets of prognostic variables, showing that moist entropy can work well as a prognostic variable in cold-cloud modeling.

a. Magnitudes of microphysical timescales

Air adjusts to saturation through vapor condensation, deposition, water evaporation or ice sublimation. Air temperature approaches 0°C through ice fusion or water freezing. Those processes are described by equations like (2.1) with two kinds of microphysical timescales. The first kind of timescales measures the adjustment to saturation. Of the timescales, the timescale for cloud water evaporation (or water vapor condensation) was discussed by Squires (1952), Politovich and Cooper (1988) and Korolev and Mazin (2003). Its expression is shown in (3.8). Its magnitude, as shown in Figure 6, is usually less than 10 seconds. The timescale for cloud ice sublimation (or water vapor deposition on cloud ice particles) was discussed by Khvorostyanov and Sassen (1998) and Korolev and Mazin (2003). Its expression is the same as that in (3.8) except that corresponding variables (e.g., a shape factor) are used. Its magnitude is larger than 10 seconds. The timescale for rainwater evaporation has the same expression as that in (3.8) except that corresponding variables are replaced and ventilation factors are introduced. With observational data (e.g., Pruppacher and Klett 1997), the timescale is estimated to be larger than 10 seconds. Similarly, the timescale for precipitating ice sublimation (or water vapor deposition on precipitating ice particles) is estimated to be larger than 10 seconds.

The second kind of timescales measures the adjustment of temperature to 0°C. The timescales are analyzed in Appendix B. Of them, the timescale for cloud ice fusion and that for precipitating ice fusion (or rainwater freezing) are much larger than 10 seconds. Since the timescale for cloud water freezing strongly depends upon the concentration of the cloud droplets with ice embryos, it may be less than 10 seconds when ice nucleus concentration is very high. For example, when temperature is lower than -40°C, all cloud

drops freeze due to homogeneous nucleation. As a result, the timescale for water cloud freezing due to homogeneous nucleation is less than 10 seconds.

Figure 6 summarizes magnitudes of the microphysical timescales scaling temperature adjustment. With the figure, prognostic variables can be chosen for the full modularization of cloud microphysics while a time step is given. If a time step is less than 0.1 second, (T, q_v, q_c) besides others can work as independent prognostic variables for the full modularization. However, if a time step is much larger than 10 seconds, it is difficult to choose independent prognostic variables for the full modularization of cloud microphysics.

If a time step is around 10 s or less, (s, q_t) besides others can work as independent prognostic variables for the full modularization of cloud microphysics and moist thermodynamics, where s and q_t exclude contributions from precipitating particles[3]. In this case, temperature is diagnosed from (s, q_t) with the procedure in Figure 2. Just as shown in section 3.b, temperature is diagnosed when s, q_t, q_i and p are given. If T<-40°C and q_c>0, cloud water freezes due to homogeneous nucleation. Assume that all cloud water freezes. Then, the air temperature T_i^* and the mixing ratio of cloud ice q_i^* are determined. If T_i^*≤-40°C, the assumption is right that all cloud water freezes. Thus q_c=0, T=T_i^*, q_i=q_i^* and q_v=q_t-q_i. If T_i^*>-40°C, the assumption is wrong. Only a part of cloud

[3] When s and q_t include contributions from precipitating particles and they are used as prognostic variables (Tripoli and Cotton 1981, 1982; Ooyama 1990, 2001), temperature is diagnosed with the procedure in Figure C-1 of Tripoli and Cotton (1982). Thus, special technologies are needed to separate (or modularize) cloud microphysics and moist thermodynamics.

water freezes. Therefore, T=-40°C, q_v=q_{vsw}, q_i is obtained easily from Equation (3.9), and q_c=q_t-q_v-q_i.

b. Microphysical processes expressed in terms of microphysical timescales

Cloud microphysics is very complicated. Some microphysical variables such as the concentration of ice particles vary in orders and some processes, such as ice nucleation and ice particle multiplication, are still unclear (e.g., Pruppacher and Klett 1997). Thus, it is interesting to confine the uncertainty of microphysics parameterization to a possible narrow extent. Microphysical timescales are important parameters in connecting cloud microphysics, moist thermodynamics and dynamics. If they are introduced to express microphysical processes, their values in modeling can be compared with those calculated from observational data as a test of cloud microphysics parameterization. Moreover, their values can be compared with the time step for integration to avoid such computational phenomenon as that in section 2. Therefore, microphysical timescales are suggested be used as intermediate variables in modeling.

This subsection presents a parcel model for cold clouds in terms of microphysical timescales, using two sets of prognostic variables, where precipitating particles move with the parcel. When one set of prognostic variables (T, p, q_v, q_c, q_r, q_i, q_s, q_g) is used, the changes of water species are described as

$$\frac{dq_v}{dt} = E_c + E_r + S_i + S_s + S_g \tag{4.1a}$$

$$\frac{dq_c}{dt} = -E_c - F_i - C_{cr} - C_{cs} - C_{cgF} - C_{cgS} \tag{4.1b}$$

$$\frac{dq_r}{dt} = -E_r - F_s - F_g + C_{cr} + C_{cgS} - C_{rgF} + C_{ir} - C_{irNrg} - C_{rsNrg} \tag{4.1c}$$

$$\frac{dq_i}{dt} = -S_i + F_i - C_{ir} - C_{is} - C_{ig} \tag{4.1d}$$

$$\frac{dq_s}{dt} = -S_s + F_s + C_{cs} + C_{is} - C_{sg} - C_{csNsg} - C_{rsNsg} \tag{4.1e}$$

$$\frac{dq_g}{dt} = -S_g + F_g + C_{ig} + C_{sg} + C_{cgF} + C_{rgF} + C_{csNsg} + C_{irNrg} + C_{rsNsg} + C_{rsNrg} \tag{4.1f}$$

where the symbols E, S, F and C indicate source terms due to evaporation, sublimation, fusion and collision, respectively.

The source terms in (4.1) are expressed next in terms of the microphysical timescales in Appendix C. Cloud water evaporation or water vapor condensation is described as

$$E_c = (q_{vsw} - q_v)/\tau_c \tag{4.2a}$$

when $q_v > q_{vsw}$ or $q_c > 0$. Otherwise, $E_c = 0$. Rainwater evaporation, cloud ice sublimation, snow sublimation and graupel sublimation are described as

$$E_r = (q_{vsw} - q_v)/\tau_r \tag{4.2b}$$

$$S_i = (q_{vsi} - q_v)/\tau_i \tag{4.2c}$$

$$S_s = (q_{vsi} - q_v)/\tau_s \tag{4.2d}$$

$$S_g = (q_{vsi} - q_v)/\tau_g, \tag{4.2e}$$

respectively, with the similar conditions for (4.2a).

With reference to Equations (B3) and (B4), the conversion of cloud water to ice is described as

$$F_i = -\frac{C_p}{L_f}\frac{T - T_o}{\tau_{ci}} + \frac{q_c}{\tau_{ci}^{(h)}} + \frac{q_c q_i}{\tau_{ciC}}, \tag{4.3a}$$

where τ_{ci} measures the timescale for cloud ice fusion when $T > T_o$ and cloud water freezing when $T < T_o$. The timescale for cloud water freezing due to homogeneous nucleation $\tau_{ci}^{(h)} = 2$ s is set when air temperature is less than –40°C. The third term on the right hand

side of (4.3a) represents the collection of cloud water by cloud ice. The fusion of snow and graupel (or rainwater freezing) are described as

$$F_s = -\frac{C_p}{L_f}\frac{T - T_o}{\tau_{rs}} \tag{4.3b}$$

$$F_g = -\frac{C_p}{L_f}\frac{T - T_o}{\tau_{rg}}, \tag{4.3c}$$

respectively.

The conversion of cloud water to rainwater due to collision is described as

$$C_{cr} = \frac{q_c q_r}{\tau_{crC}} + \max\left\{\frac{q_c - q_{cA}}{\tau_{crA}}, 0\right\}, \tag{4.4}$$

where the two terms on the right hand side represent the collection of cloud water by rainwater and cloud water autoconversion, respectively. The conversion of cloud ice to snow due to aggregation, deposition and riming is described as

$$C_{is} = \frac{q_i q_s}{\tau_{isC}} + \max\left\{\frac{q_v - q_{vsi}}{\tau_{iNis}}, 0\right\} + \frac{q_i q_c}{\tau_{ciNis}}, \tag{4.5}$$

where the first term on the right hand side represents the collection of cloud ice by snow, and the second and the third terms represent the conversion of cloud ice to snow due to vapor deposition and the collection of cloud water, respectively.

When graupel particles collect cloud drops, a part of water freezes around the particles and the other part sheds off the particles as raindrops when T<0°C. Thus, the conversion of cloud water to graupel is described as

$$C_{cgF} = \min\left\{\frac{q_c q_g}{\tau_{cgC}}, \frac{C_p(T_o - T)}{L_f \tau_{cgF}}\right\}, \tag{4.6a}$$

where the first term in the brackets represents all cloud water collected by graupel and the second term represents a part of cloud water that freezes. The other part of cloud water that sheds off graupel as rainwater is described as

$$C_{cgS} = \max\left\{\frac{q_c q_g}{\tau_{cgC}} - \max[\frac{C_p(T_o - T)}{L_f \tau_{cgF}}, 0], 0\right\}. \tag{4.6b}$$

The preceding equation is also suitable for the shedding of accreted water when $T \geq 0°C$. Similarly, the conversion of rainwater to graupel due to the collection of rainwater by graupel is described as

$$C_{rgF} = \min\left\{\frac{q_r q_g}{\tau_{rgC}}, \frac{C_p(T_o - T)}{L_f \tau_{rgF}}\right\}. \tag{4.7}$$

Owing to the collection of cloud water by snow, the conversion of cloud water to snow is described as

$$C_{cs} = \frac{q_c q_s}{\tau_{csC}}, \tag{4.8a}$$

and the conversion of snow to graupel as

$$C_{csNsg} = \frac{q_c q_s}{\tau_{csNsg}}. \tag{4.8b}$$

Due to the collection of cloud ice by rainwater, cloud ice is converted to rainwater with the rate

$$C_{ir} = \frac{q_i q_r}{\tau_{irC}}, \tag{4.9a}$$

and rainwater is converted to graupel with the rate

$$C_{irNrg} = \frac{q_i q_r}{\tau_{irNrg}}. \tag{4.9b}$$

Exactly speaking, the real rate for the conversion of rainwater to graupel is C_{irNrg}-C_{ir} when air temperature is below 0°C.

The conversions of snow and rainwater to graupel due to the collection of snow by rainwater are described as

$$C_{rsNsg} = \frac{q_s q_r}{\tau_{rsNsg}} \tag{4.10a}$$

$$C_{rsNrg} = \frac{q_s q_r}{\tau_{rsNrg}}, \tag{4.10b}$$

respectively. The conversions of cloud ice and snow to graupel due to the collection of cloud ice and snow by graupel are described as

$$C_{ig} = \frac{q_i q_g}{\tau_{igC}} \tag{4.11a}$$

$$C_{sg} = \frac{q_s q_g}{\tau_{sgC}}, \tag{4.11b}$$

respectively.

Equations (4.2)-(4.11) express microphysical processes in terms of microphysical timescales. They are equivalent to the current schemes for cloud microphysics parameterization (e.g., Lin *et al.* 1983; Rutledge and Hobbs 1984; Tao *et al.* 1993; Ferrier 1994; Ferrier *et al.* 1995) when the timescales take corresponding expressions. Next, a set of microphysical timescales in Table 1 is taken simply for a numerical test of prognostic variables.

Table 1 Microphysical Timescales in a Parcel Model

Condensation/Sublimation		Fusion/Freezing		Collision	
τ_c	3	τ_{ci}	$10^3(q_{ref}/q_i)$ when $T>T_o$	τ_{crC}	0.2
τ_i	3×10^3		$10^3(q_{ref}/q_c)$ when $T<T_o$	τ_{crA}	10^3
τ_r	$3\times10^3(q_{ref}/q_r)^{1/2}$	τ_{rs}	$10^3(q_{ref}/q_s)^{1/2}$ when $T>T_o$	τ_{cgF}	10^3
τ_s	$3\times10^4(q_{ref}/q_s)^{1/2}$		$10^3(q_{ref}/q_r)^{1/2}$ when $T<T_o$	τ_{cgC}	0.2
τ_g	$3\times10^4(q_{ref}/q_g)^{1/2}$	τ_{rg}	$10^3(q_{ref}/q_g)^{1/2}$ when $T>T_o$	τ_{rgF}	10^3
			$10^3(q_{ref}/q_r)^{1/2}$ when $T<T_o$	τ_{rgC}	2
				τ_{csC}	0.7
				τ_{ciC}	4
				τ_{isC}	1.5
				τ_{irC}	0.2
				τ_{igC}	5
				τ_{sgC}	8
τ_{iNis}	10^3	$\tau_{ci}^{(h)}$	2	τ_{csNsg}	1.5
				τ_{ciNis}	3
				τ_{irNrg}	1
				τ_{rsNsg}	1
				τ_{rsNrg}	2

c. Two sets of prognostic variables for cold clouds

When one set of prognostic variables (T, p, q_v, q_c, q_r, q_i, q_s, q_g) is used, the governing equations for the parcel are Equation (4.1) for mixing ratios, (3.17) for pressure and the following energy equation for temperature

$$\begin{aligned}&(C_p + C_{pv}q^*)\frac{dT}{dt} - R_dT\frac{d\ln(p-e)}{dt} - q_vR_vT\frac{d\ln e}{dt}\\ &= L_f(F_i + F_t + C_{cgF} + C_{cs}) - L_v(E_c + E_r) - L_s(S_i + S_s + S_g)\end{aligned}, \tag{4.12}$$

where the symbols

$$F_t = F_s + F_g + C_{rgF} + C_{irNrg} - C_{ir} + C_{rsNrg} \tag{4.13a}$$

$$q^* = q_v + C_{pv}^{-1}\left[c_l(q_c + q_r) + c_i(q_i + q_s + q_g)\right]. \tag{4.13b}$$

When the other set of prognostic variables (s, p, q_t, q_r, q_i, q_s, q_g) is used, the governing equations for the parcel are the same as those for the first set of prognostic variables

except for those for q_t and s. The equation for q_t the mixing ratio of airborne water is obtained from Equations (4.1a), (4.1b) and (4.1d), or

$$\frac{dq_t}{dt} = E_r + S_s + S_g - C_{cr} - C_{cs} - C_{cgF} - C_{cgS} - C_{ir} - C_{is} - C_{ig} \tag{4.14}$$

The equation for moist entropy is obtained from the energy equation (Zeng *et al.* 2005), or

$$\begin{aligned}\frac{ds}{dt} &= \frac{L_f(F_t - S_t + C_{ip})}{T} + c_l(E_t + S_t - C_{ip})\ln\frac{T}{T_{ref}} \\ &+R_v(F_i - S_i - C_{ip})\ln\frac{E_{sw}}{E_{si}} - R_v(E_t + S_t + S_i - F_i)\ln f \\ &-\frac{c_l q_r + c_i(q_s + q_g)}{T}\frac{L_f F_t - L_v E_t - L_s(S_t + S_i - F_i) - R_d T\lambda_p^{-1}}{C_{\tilde{p}} + C_{pv}q^*}\end{aligned} \tag{4.15a}$$

when air is unsaturated with respect to water and

$$\begin{aligned}\frac{ds}{dt} &= \frac{L_f(F_t - S_t + C_{cp} + C_{ip})}{T} + c_l(S_t - C_{cr} - C_{cp} - C_{ip})\ln\frac{T}{T_{ref}} \\ &+R_v(F_i - S_i - C_{ip})\ln\frac{E_{sw}}{E_{si}} - \frac{c_l q_r + c_i(q_s + q_g)}{T} \\ &\left[L_f(F_i + F_t + C_{cp} - S_i - S_t) - (R_d T + L_v q_{vsw})\lambda_p^{-1}\right]\left[C_p + C_{pv}q^* + (1 + \frac{R_v}{R_d}q_{vsw})\frac{L_v^2 q_{vsw}}{R_v T^2}\right]^{-1}\end{aligned} \tag{4.15b}$$

when air is saturated with respect to water, where

$$S_t = S_s + S_g \tag{4.16a}$$

$$C_{cp} = C_{cr} + C_{cgS} \tag{4.16b}$$

$$C_{ip} = C_{is} + C_{ig} + C_{ir} \tag{4.16c}$$

$$\lambda_p^{-1} = -\frac{dp}{(p - e)dt}. \tag{4.16d}$$

Just as done in section 3.c, numerical results from the parcel model are compared when two sets of prognostic variables are used, reaching the same conclusion as that in section 3.c. The parcel model takes the same numerical scheme as that in (2.2). Suppose

that the air parcel moves upward with a vertical velocity of w=4 m/s as well as an initial pressure 1000 hpa, relative humidity of 60% and temperature of 300 K. Numerical results from the model with the two sets of prognostic variables are displayed in Figure 7. In the figure, thin solid lines display the results from the model with Δt=0.1 s and the first set of prognostic variables, and thick dashed lines display the results from the model with Δt=10 s and the second set of prognostic variables. As shown in the figure, the results with the two sets of prognostic variables agree well, showing that the moist entropy can work well as a prognostic variable in the modeling of cold clouds.

5. Summary

Cloud microphysics is very complicated. Its many variables (e.g, the concentrations of ice nuclei and particles) vary in orders, and some processes (e.g., ice particle multiplication) are still unclear (e.g., Pruppacher and Klett 1997). Thus, a proper parameterization scheme for cloud microphysics possesses not only complicated formulas but also uncertain factors. To confine the uncertainty of cloud microphysics parameterization to a possible narrow extent and limit the computational feedback between cloud microphysics and dynamics, the paper suggests that microphysical timescales be introduced in cloud-resolving models as intermediate variables.

Microphysical timescales are important parameters in connecting cloud microphysics, thermodynamics and dynamics. They are determined by microphysical variables[4]. Thus,

[4] For the brevity of model formulation, microphysical timescales are defined in the present paper as functions of microphysical variables such as those in Eqs. (3.8) and (B2), measuring the adjustments to saturation and 0°C as well as the conversion between hydrometeor species due to

the issue of cloud microphysics parameterization is how to formulate them for cloud-resolving modeling. If the timescales are introduced as intermediate variables, they can benefit the modeling of cloud microphysics. Their values in modeling can be compared with those calculated with observational data as a test of microphysics parameterization, especially for a specific cloud. Moreover, their values in modeling can be compared with the time step for numerical integration, judging whether microphysical processes are represented properly in the discretization of differential equations.

Magnitudes of the microphysical timescales scaling temperature adjustment, on the basis of previous work (Squires 1952; Politovich and Cooper 1988; Khvorostyanov and Sassen 1998; Korolev and Mazin 2003) and Appendix B, are surveyed against a time step in the present paper. Of all timescales analyzed, the timescale for cloud water evaporation and that for cloud water freezing due to homogeneous nucleation are around 1 second. Others are longer than 10 seconds. As a special case, when plenty of artificial ice nuclei are introduced in clouds suddenly, the timescale for water freezing may approach one second.

Independent microphysical prognostic variables are suggested be used for the modularization of cloud microphysics. On the basis of the magnitudes of microphysical timescales, moist entropy is proposed be used as a prognostic variable in place of temperature, and temperature is diagnosed from moist entropy and other prognostic

---

collision, respectively. As a contrast, a complex timescale for phase relaxation (e.g., Khvorostyanov and Sassen 1998; Korolev and Mazin 2003) can be introduced to measure the approach to saturation in a parcel model. It depends on not only microphysical but also dynamic variables.

variables. Different from that used in other similar models (Tripoli and Cotton 1981; Ooyama 1990), the moist entropy proposed here has no contributions from precipitating particles for easy diagnosis of temperature and full modularization of cloud microphysics.

Air parcels in adiabatic upward motion are simulated with two sets of independent prognostic variables, showing the benefit of using moist entropy as a prognostic variable. The first set of prognostic variables is (T, q_v, q_c), involving no assumption of zero supersaturation. When the time step is small (e.g., less than 1 s), numerical results are reasonable. When the time step is large (e.g., larger than 2 s), numerical results are overwhelmed with great computational errors, exhibiting the phenomena of spurious supersaturation and negative mixing ratio of cloud water. The second set of prognostic variables is (s, q_t), accompanying the assumption of zero supersaturation. When the time step is 10 s or around, numerical results agree well with those using the first set of prognostic variables and a very small time step (e.g., 0.1 s). The comparison of the two sets of prognostic variables shows clearly that, if prognostic variables are independent, (s, q_t) work more efficiently than (T, q_v, q_c) as prognostic variables in cloud-resolving modeling.

Acknowledgements. The work is supported by the NASA Headquarters Atmospheric Dynamics and Thermodynamics Program and the NASA Tropical Rainfall Measuring Mission (TRMM). The authors are grateful to Dr. R. Kakar at NASA headquarters for his support of this research. They thank Mr. S. Lang for reading the manuscript.

APPENDIX A

List of Symbols

A_w : defined in (3.3)

$C_p/C_{pv}/c_l$: specific heat of dry air/water vapor/liquid water

C_{cp} : conversion of cloud water to precipitating ice

C_{ip} : conversion of cloud ice to precipitating ice

C_{cr} : conversion of cloud water to rainwater due to collision

C_{is} : conversion of cloud ice to snow due to aggregation, deposition and riming

C_{cgF}/C_{cgS} : freezing/shedding part in the collection of cloud water by graupel

C_{rgF} : freezing part in the collection of rainwater by graupel

C_{cs} : collection of cloud water by snow

C_{csNsg} : conversion of snow to graupel due to the collection of cloud water by snow

C_{ir} : collection of cloud ice by rainwater

C_{irNrg} : conversion of rainwater to graupel due to the collection of cloud ice by rainwater

C_{rsNsg} : conversion of snow to graupel due to the collection of rainwater by snow

C_{rsNrg} : conversion of rainwater to graupel due to the collection of rainwater by snow

C_{ig}/C_{sg} : collection of cloud ice/snow by graupel

D_v : coefficient of water vapor diffusion in air

e : partial pressure of water vapor

E_c/E_r : evaporation of cloud water /rainwater

E_{sw}/E_{si} : saturation vapor pressure over water/ice

$f=e/E_{sw}$: relative humidity

F_i : conversion of cloud water to cloud ice

F_s/F_g : conversion between rainwater and snow/graupel due to fusion or freezing

F_t : total conversion of rainwater to precipitating ice, see (4.13a)

g : acceleration due to gravity

K_a : coefficient of air heat conductivity

$L_v/L_s/L_f$: latent heat of vaporization/sublimation/freezing

N_c/ N_i : concentration of cloud droplets/ cloud ice particles

p : total pressure of moist air

$p_{ref}=10^5$ pa : reference pressure

q_{vsw}/q_{vsi} : saturation mixing ratio of water vapor over water/ice

$q_v/q_c/q_i/q_r/q_s/q_g$: mixing ratio of water vapor/cloud water/cloud ice/rain/snow/graupel

$q_t=q_v+q_c+q_i$: total mixing ratio of airborne water

$r_c/ /r_i/$: radius of cloud droplets/ cloud ice particles

R_d/R_v : gas constant of dry air/water vapor

s : moist entropy per unit mass

s_w : supersaturation of water vapor, see (3.11)

$S_i/S_s/S_g$: sublimation of cloud ice/snow/graupel

S_t : total sublimation of precipitating ice

t : time

T : temperature

$T_o=273.15$ K : absolute temperature at the melting point

$T_{ref}=273.15$ K : reference temperature

w : vertical velocity

z : height

τ : timescale

$\tau_c/\tau_i/\tau_r/\tau_s/\tau_g$: timescale for the evaporation or sublimation of cloud water/cloud ice/rainwater/snow/graupel

τ_{iNis} : timescale for the conversion of cloud ice to snow due to deposition

$\tau_{ci}/\tau_{rs}/\tau_{rg}$: fusion or freezing timescale for the conversion from cloud water to cloud ice/rainwater to snow/rainwater to graupel

$\tau_{ci}^{(h)}$: timescale of cloud water freezing due to homogeneous nucleation

$\tau_{crC}/\tau_{cgC}/\tau_{rgC}/\tau_{csC}/\tau_{ciC}/\tau_{isC}/\tau_{irC}/\tau_{igC}/\tau_{sgC}$: timescale for the collection of cloud water by rainwater/cloud water by graupel/rainwater by graupel/cloud water by snow/cloud water by cloud ice/cloud ice by snow/cloud ice by rainwater/cloud ice by graupel/snow by graupel

τ_{crA} : timescale for the autoconversion of cloud water to rainwater

τ_{cgF}/τ_{rgF} : freezing timescale in the collection of cloud water/rainwater by graupel

$\tau_{csNsg}/\tau_{ciNis}/\tau_{irNrg}/\tau_{rsNsg}/\tau_{rsNrg}$: timescale for the conversion from snow to graupel/cloud ice to snow/rainwater to graupel/snow to graupel/rainwater to graupel due to the collection of cloud water by snow/cloud water by cloud ice/cloud ice by rainwater/rainwater by snow/rainwater by snow

Δt : time step for numerical integration

ρ : air density

ρ_w/ρ_i : density of liquid water/ice

APPENDIX B

Timescales for Ice Fusion

This appendix deals with the timescales for ice fusion or water freezing. Consider an air parcel that is adiabatic and stationary (or w=0). Assume for simplicity that particles are spherical ice and monodispersely distributed. No liquid water surrounds the ice particles. Let the symbols N_i and r_i denote the concentration and the radius of ice particles, respectively. Since heat is transferred from air to ice particles for ice fusion, air temperature is decreased, which is described as

$$C_p \frac{dT}{dt} = -4\pi r_i f_h K_a \frac{N_i}{\rho}(T - T_o). \tag{B1}$$

Water vapor may condense at the surface of the ice particles. The resulting latent heat is balanced by a part of the latent heat of ice melting, without changing air temperature directly. Thus, no term in the preceding equation expresses directly water vapor condensation or water evaporation at the surface of the ice particles.

As shown in Equation (B1), air temperatures approaches 0°C with a timescale

$$\tau = \frac{\rho C_p}{4\pi f_h K_a N_i r_i}. \tag{B2}$$

Using the timescale, (B1) is rewritten for ice fusion as

$$\frac{dq_i}{dt} = -\frac{C_p}{L_f}\frac{T - T_o}{\tau}. \tag{B3}$$

With the expression (B2), the timescale for cloud ice fusion is estimated and its magnitude is shown in Figure 6. Similar discussions are suitable for the fusion of precipitating ice.

The expression (B2) is also suitable for the freezing of water when N_i and r_i are replaced with the concentration of the cloud drops with ice embryos and the radius of the cloud drops, respectively. Obviously, the timescale for ice freezing depends strongly upon the concentration of the cloud drops with ice embryos, and ice nucleation processes control the latter. Figure 6 displays the possible extent of the timescale for cloud water freezing.

When air temperature is lower than -40°C, all cloud drops freeze due to homogeneous ice nucleation. Thus the timescale in (B2) is small, close to one second. Since the relative change of q_i is larger than that of $(T\text{-}T_0)$, Equation (B1) can be rewritten as

$$\frac{dq_c}{dt} = -\frac{q_c}{\tau^{(h)}} \tag{B4}$$

for the freezing due to homogeneous nucleation, where

$$\tau^{(h)} = \frac{L_f r_i^2}{3 f_h K_a (T - T_o)}. \tag{B5}$$

In contrast to the timescale in (B2), the timescale in (B5) measures the decrease of cloud water due to homogeneous nucleation freezing. Since $\tau^{(h)} << \tau$, both $\tau^{(h)}$ and τ are small in magnitude, implying that T and q_i change *rapidly* with time due to homogeneous nucleation. Hence, a special numerical technique is needed for efficient modeling (see Figure 2 for details).

APPENDIX C

Confines of Microphysical Timescales

When microphysical timescales are used as intermediate variables in modeling, their values can be compared with those calculated from observational data, confining the uncertainty of cloud microphysics parameterization. Their values can also be compared with the time step for explicit integration, avoiding computational instability. This appendix deals with the comparison of microphysical timescales against the time step.

Of all the timescales in Equations (4.1)-(4.11), the timescale in (4.2a) for cloud water evaporation or water vapor condensation is expressed as

$$\tau_c = \frac{\rho q_{vsw}}{4\pi\rho_w A_w f_v N_c \bar{r}_c} \tag{C1}$$

where $\bar{r}_c$ is the averaged radius of cloud droplets and f_v is a ventilation factor. Obviously, τ_c is different from that in Equation (3.8) by a factor

$$(1 + \frac{q_{vsw} L_v^2}{R_v C_p T^2}) . \tag{C2}$$

With the analysis in sections 2 and 3, the computational criterion for this process is written as

$$\tau_c > (1 + \frac{q_{vsw} L_v^2}{R_v C_p T^2})\Delta t . \tag{C3}$$

Similarly, other timescales τ_r, τ_i, τ_s and τ_g in (4.2) have the same characteristics as those in (C1)-(C3) except that corresponding variables are replaced.

The timescale for cloud ice fusion or cloud water freezing τ_{ci} measures temperature adjustment. As shown in Equations (B1) and (B2), the computational criterion for cloud ice fusion (or cloud water freezing) is written as

$$\tau_{ci} > \Delta t. \tag{C4}$$

Other timescales for fusion or freezing (τ_{rs}, τ_{rg}, τ_{cgF} and τ_{rgF}) have the same computational criterion. Although the timescale $\tau_{ci}^{(h)}$ measures the decrease of cloud water due to homogeneous nucleation freezing, it has the similar computational criterion as (C4), as shown in (B4).

The timescale τ_{crC} is used to describe the collection of cloud water by rainwater as

$$\frac{dq_c}{dt} = -\frac{q_c q_r}{\tau_{crC}} \tag{C5}$$

The computational criterion for explicit integration of (C5) is

$$\tau_{crC} > q_r \Delta t. \tag{C6}$$

Similarly, other timescales for collection growth (e.g., τ_{csC}, τ_{cgC}, τ_{ciC}, τ_{irC}, τ_{isC}, τ_{igC}, τ_{sgC} and τ_{rgC}) have the same computational criterion except that corresponding variables are replaced.

Once a computation criterion in (C3), (C4) or (C6) is violated, the time step for integration needs to be decreased. Otherwise, special modeling techniques need to be introduced to resolve the computational issue (e.g., Tao, Simpson and McCumber, 1989; Grabowski and Smolarkiewicz 1990; Margolin *et al.* 1997).

REFERENCES

Albrecht, B. and S. K. Cox, 1975: The large-scale response of the tropical atmosphere to cloud-modulated infrared heating. *J. Atmos. Sci.*, **32**, 16-24.

Baker, M. B., 1997: Cloud microphysics and climate. *Science*, **276**, 1072-1078.

Cotton, W. R., R. A. Pielke Sr., R. L. Walko, G. E. Liston, C. J. Tremback, H. Jiang, R. L. McAnelly, J. Y. Harrington, M. E. Nicholls, G. G. Carrio and J. P. McFadden, 2003: RAMS 2001: Current status and future directions. *Meteor. Atmos. Phys.*, **82**, 5-29.

Ferrier, B. S., 1994: A double-moment multiple-phase four-class bulk ice scheme. Part I: Description. *J. Atmos. Sci.*, **51**, 249-280.

Ferrier, B. S., W.-K. Tao and J. Simpson, 1995: A double-moment multiple-phase four-class bulk ice scheme. Part II: Simulations of convective storms in different large-scale environments and comparisons with other parameterizations. *J. Atmos. Sci.*, **52**,1001-1033.

Grabowski, W. W., 1989: Numerical experiments on the dynamics of the cloud-environment interface: small cumulus in a shear-free environment. *J. Atmos. Sci.*, **46**, 3513-3541.

Grabowski, W. W. and P. K. Smolarkiewicz, 1990: Monotone finite-difference approximations to the advection-condensation problem. *Mon. Wea. Rev.*, **118**, 2082-2097.

Khvorostyanov, V. I. And K. Sassen, 1998: Cirrus cloud simulation using explicit microphysics and radiation. Part I: Model description. *J. Atmos. Sci.*, **55**, 1808-1821.

Klemp, J. B. and R. B. Wilhelmson, 1978: The simulation of three-dimensional convective storm dynamics. *J. Atmos. Sci.*, **35**, 1070-1096.

Korolev, A. V. and I. P. Mazin, 2003: Supersaturation of water vapor in clouds. *J. Atmos. Sci.*, **60**, 2957-2974.

Lin, Y.-L., R. D. Farley and H. D. Orville, 1983: Bulk parameterization of the snow field in a cloud model. *J. Clim. Appl. Meteor.*, **22**, 1065-1092.

Margolin, L., J. M. Reisner and P. K. Smolarkiewicz, 1997: Application of the volumn-of-fluid method to the advection-condensation problem. *Mon. Wea. Rev.*, **125**, 2265-2273.

Ooyama, K. V., 1990: A thermodynamic foundation for modeling the moist atmosphere. *J. Atmos. Sci.*, **47**, 2580-2593.

Ooyama, K. V., 2001: A dynamic and thermodynamic foundation for modeling the moist atmosphere with parameterized microphysics. *J. Atmos. Sci.*, **58**, 2073-2102.

Politovich, M. K. and W. A. Cooper, 1988: Variability of the supersaturation in cumulus clouds. *J. Atmos. Sci.*, **45**, 1651-1664.

Pruppacher, H. R. and J. D. Klett, 1997: *Microphysics of clouds and precipitation.* Kluwer, 954 pp.

Raymond, D. J., 2000: The Hadley circulation as a radiative-convective instability. *J. Atmos. Sci.*, **57**, 1286-1297.

Raymond, D. J. and A. M. Blyth, 1986: A stochastic mixing model for nonprecipitating cumulus clouds. *J. Atmos. Sci.*, **43**, 2708-2718.

Raymond, D. J. and X. Zeng, 2000: Instability and large-scale circulations in a two-column model of the tropical troposphere. *Quart. J. Roy. Meteor. Soc.*, **126**, 3117-3135.

Riehl, H. and J. S. Malkus, 1958: On the heat balance in the equatorial trough zone. *Geophysica*, **6**, 503-538.

Rutledge, S. A. and P. V. Hobbs, 1984: The mesoscale and microscale structure and organization of clouds and precipitation in mid-latitude clouds. Part XII: A diagnostic modeling study of precipitation development in narrow cold frontal rainbands. *J. Atmos. Sci.*, **41**, 2949-2972.

Simpson, J., R. F. Adler and G. R. North, 1988: A proposed Tropical Rainfall Measuring Mission (TRMM) satellite. *Bull. Amer. Meteor. Soc.*, **69**, 278-295.

Smolarkiewicz, P. K., 1983: A simple positive definite advection scheme with small implicit diffusion. *Mon. Wea. Rev.*, **111**, 479-486.

Squires, P., 1952: The growth of cloud drops by condensation. *Aust. J. Sci. Res.*, **5**, 59-86.

Tao, W.-K. and R. Adler, 2003a: Cloud systems, hurricanes, and the Tropical Rainfall Measuring Mission (TRMM). *Meteor. Monogr.*, No. 51, Amer. Meteor. Soc., 234pp.

Tao, W.-K., J. Simpson, D. Baker, S. Braun, M.-D. Chou, B. Ferrier, D. Johnson, A. Khain, S. Lang, B. Lynn, C.-L. Shie, D. Starr, C.-H. Sui, Y. Wang and P. Wetzel, 2003b: Microphysics, radiation and surface processes in the Goddard Cumulus Ensemble (GCE) model. *Meteor. Atmos. Phys.*, **82**, 97-137.

Tao, W.-K. and J. Simpson, 1993: The Goddard Cumulus Ensemble model. Part I: Model description. *Terr. Atmos. Oceanic Sci.*, **4**, 19-54.

Tao, W.-K., J. Simpson and M. McCumber, 1989: An ice-water saturation adjustment. *Mon. Wea. Rev.*, **117**, 232-235.

Tompkins A. M. and G. C. Craig, 1998: Radiative-convective equilibrium in a three-dimensional cloud ensemble model. *Quart. J. Roy. Meteor. Soc.*, **124**, 2073-2098.

Tripoli, G. J. and W. R. Cotton, 1981: The use of ice-liquid water potential temperature as a thermodynamic variable in deep atmospheric models. *Mon. Wea. Rev.*, **109**, 1094-1102.

Tripoli, G. J. and W. R. Cotton, 1982: The Colorado State University three-dimensional cloud/mesoscale model —— 1982 Part I: General theoretical framework and sensitivity experiments. *J. Rech. Atmos.*, **16**, 185-219.

Zeng, X., 2001: *Ensemble simulation of tropical convection.* Ph.D. dissertation, New Mexico Tech. New Mexico Tech Library, 124pp.

Zeng, X., W.-K. Tao and J. Simpson, 2005: An equation for moist entropy in a precipitating and icy atmosphere. *J. Atmos. Sci.*, 62, 4293-4309.

Figure Captions

Figure 1 The timescale of water vapor condensation varies with pressure (or temperature). The results with $N_c r_c$= 500 and 3000 $\mu m \cdot cm^{-3}$ are displayed with thin and thick lines, respectively.

Figure 2 Schematic on the diagnosis of temperature from the moist entropy and the total mixing ratio of airborne water.

Figure 3 Change in output variables with height while two sets of prognostic variables are used. Thin solid lines display the variables from the model with Δt=0.1 s and the first set of prognostic variables (T, q_v, q_c); thin dashed lines display those from the model with Δt=3 s and the first set of prognostic variables (T, q_v, q_c); and thick dashed lines display those from the model with Δt=10 s and the second set of prognostic variables. Thin solid lines coincide with thick dashed lines.

Figure 4 Variables at t=10 minutes vary with height when the first set of prognostic variables (T, q_v, q_c) and an upstream scheme are used. Dashed thick lines display analytical results. Solid and dashed thin lines display the variables from the model with Δt=0.1 and 3 s, respectively.

Figure 5 the same as Figure 4 except for Δt=10 s and the second set of prognostic variables (s, q_t). Solid and dashed thin lines display the variables from the model with an upstream scheme and the Smolarkiewicz scheme, respectively.

Figure 6 Magnitudes of the microphysical timescales scaling temperature adjustment.

Figure 7 Change in output variables with height while two sets of prognostic variables are used. Thin solid lines display the variables from the model with Δt=0.1 s and the first set of prognostic variables (or T and others); and thick dashed lines display those from the model with Δt=10 s and the second set of prognostic variables (or s and others).

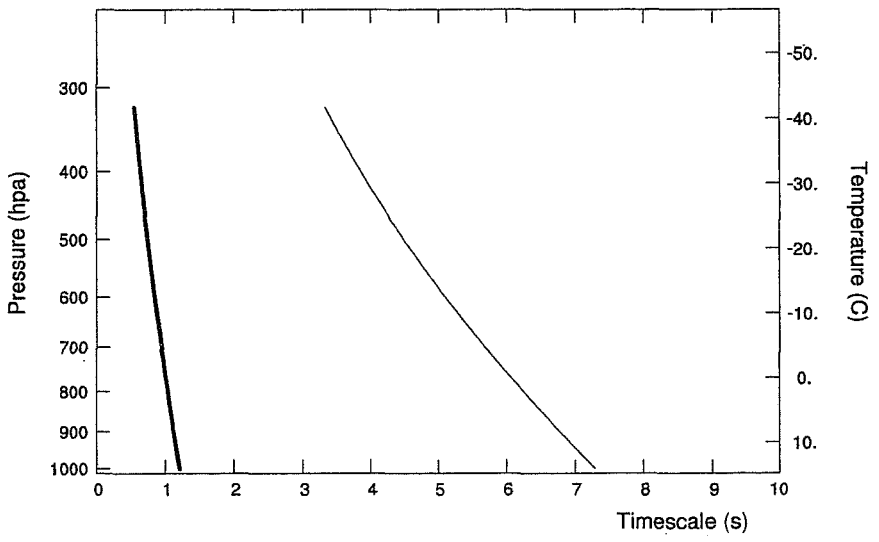

Figure 1 The timescale of water vapor condensation varies with pressure (or temperature). The results with $N_c r_c$= 500 and 3000 μm·cm^{-3} are displayed with thin and thick lines, respectively.

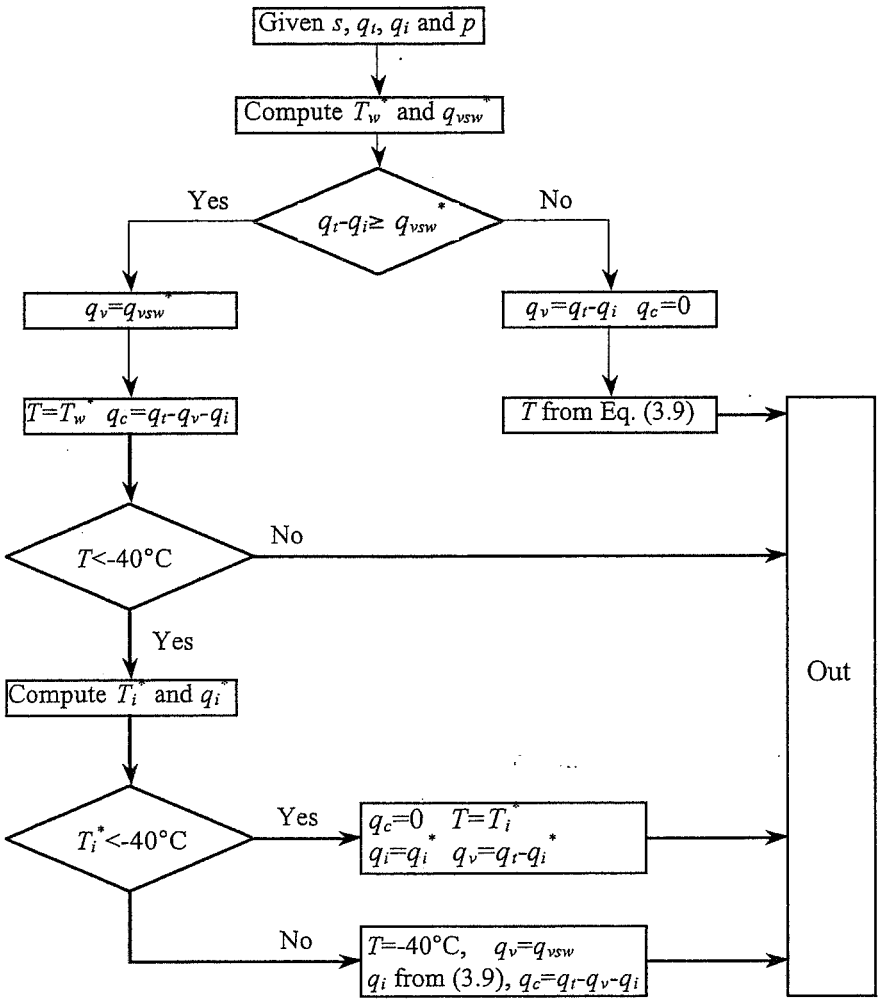

Figure 2 Schematic on the diagnosis of temperature from the moist entropy and the total mixing ratio of airborne water.

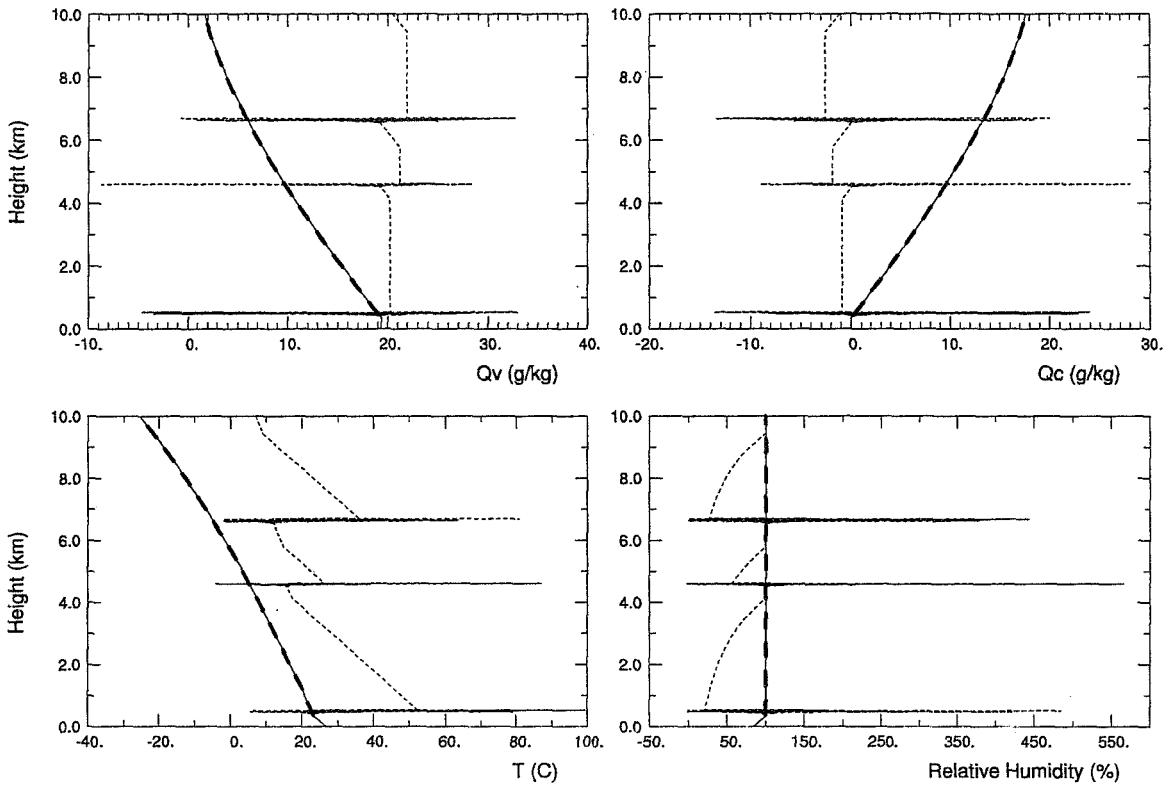

Figure 3 Change in output variables with height while two sets of prognostic variables are used. Thin solid lines display the variables from the model with Δt=0.1 s and the first set of prognostic variables (T, q_v, q_c); thin dashed lines display those from the model with Δt=3 s and the first set of prognostic variables (T, q_v, q_c); and thick dashed lines display those from the model with Δt=10 s and the second set of prognostic variables. Thin solid lines coincide with thick dashed lines.

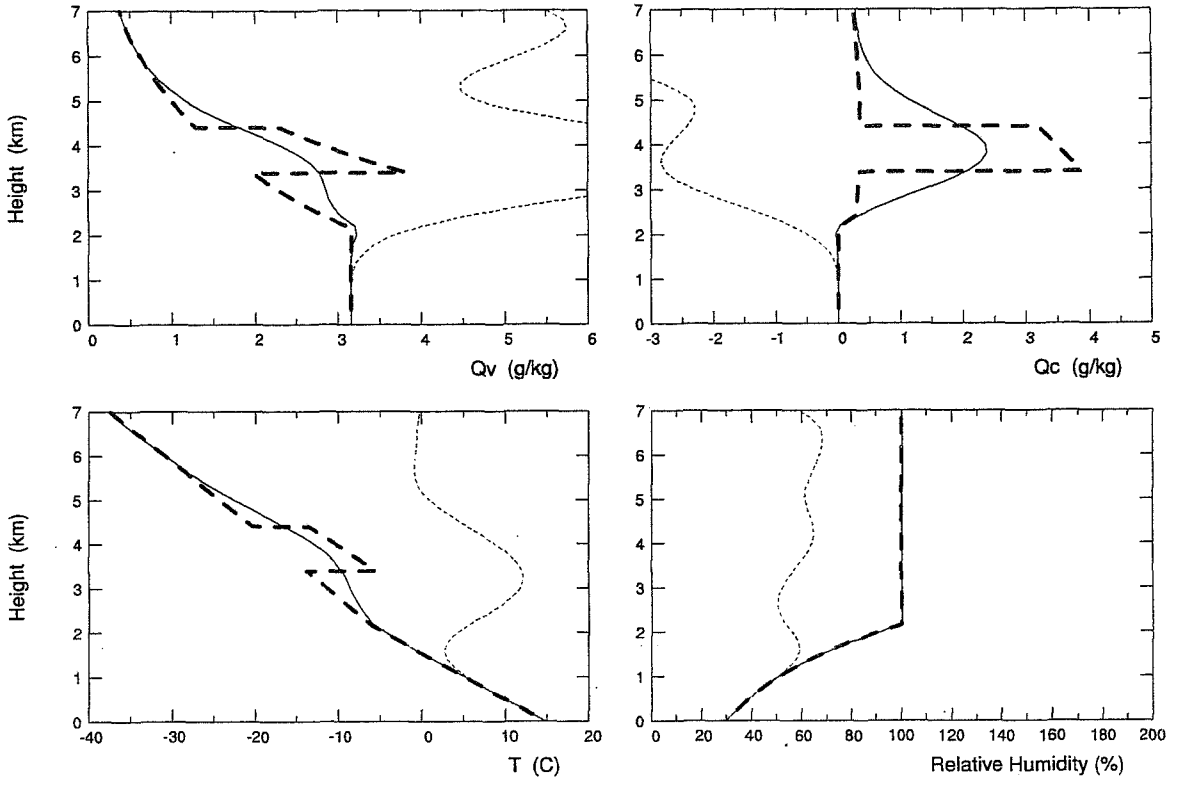

Figure 4 Variables at t=10 minutes vary with height when the first set of prognostic variables (T, q_v, q_c) and an upstream scheme are used. Dashed thick lines display analytical results. Solid and dashed thin lines display the variables from the model with Δt=0.1 and 3 s, respectively.

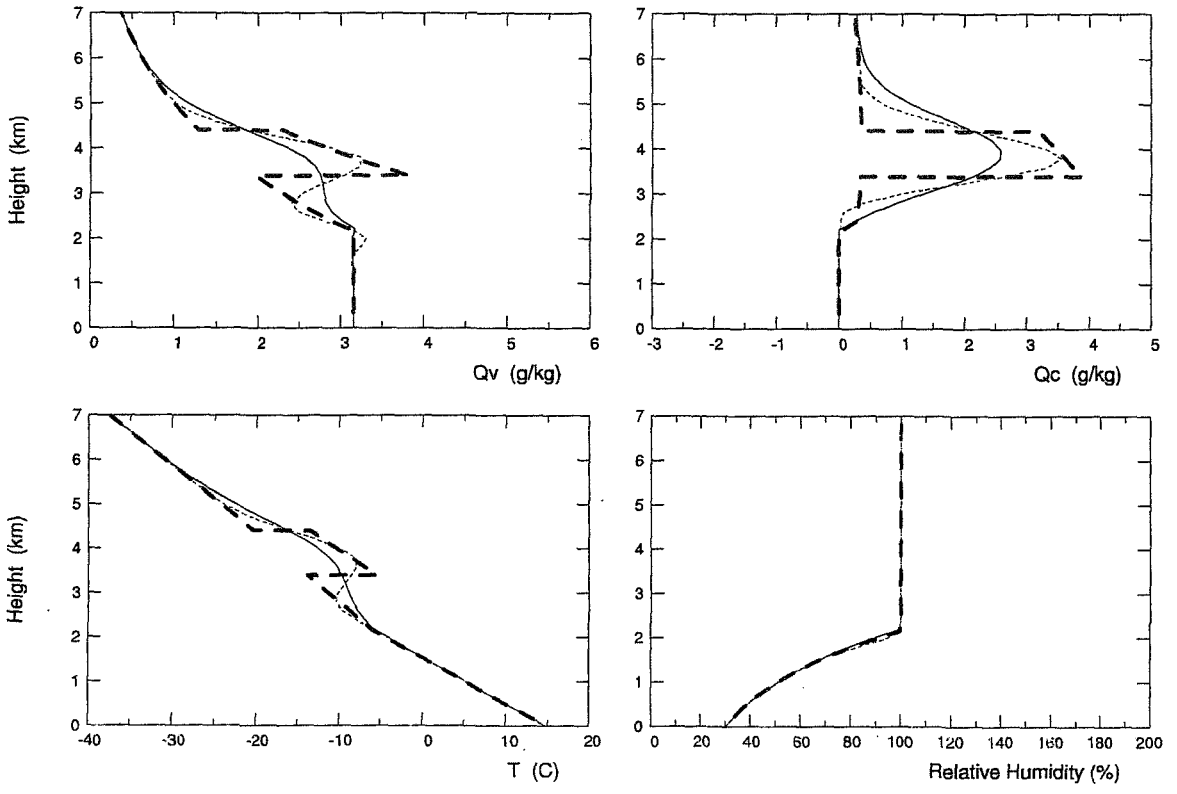

Figure 5 the same as Figure 4 except for Δt=10 s and the second set of prognostic variables (s, q_t). Solid and dashed thin lines display the variables from the model with an upstream scheme and the Smolarkiewicz scheme, respectively.

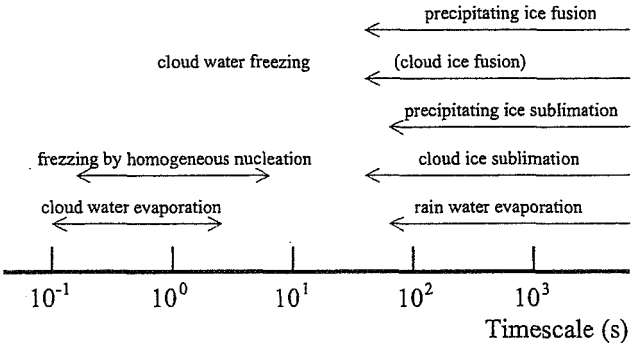

Figure 6 Magnitudes of the microphysical timescales scaling temperature adjustment.

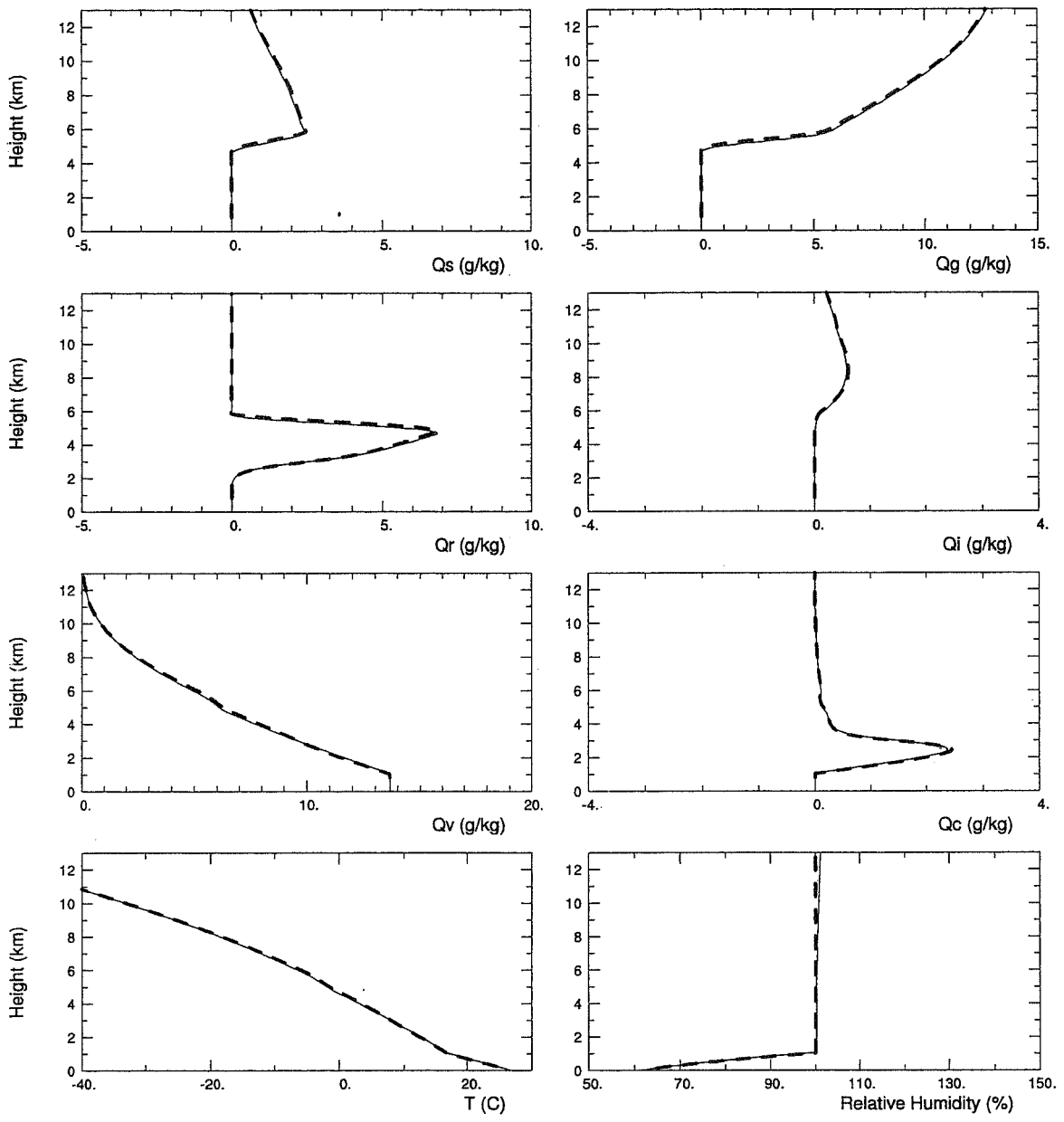

Figure 7 Change in output variables with height while two sets of prognostic variables are used. Thin solid lines display the variables from the model with Δt=0.1 s and the first set of prognostic variables (or T and others); and thick dashed lines display those from the model with Δt=10 s and the second set of prognostic variables (or s and others).